

Hiromi SENO · Naoki SATO

## Mathematical Models for Epidemic Dynamics with Adult Vaccination against Waning Immunity

### 免疫失活に対する成人ワクチン接種を伴う伝染病感染動態に関する数理モデル

Version date: December 20, 2004

**Abstract.** We analyze two simple mathematical models taking account of the waning immunity, specifically formulated with measles in mind, to give some insight about the effect of vaccination in adult age class according to the elimination of measles within the whole population. First model is non-age-structured one, and the second model is with three age classes: infant, young, and adult. With mathematical and numerical analyses making use of parameter values which could correspond to the demographic situation of a Japanese community, we show the result emphasizing that the vaccination program should be planned with taking account of the size of population within which the disease transmission is taking place. Especially in case of Japan, although our numerical calculations imply that it would be hard to increase the infant vaccination rate enough to make the population approach the disease-free equilibrium, the increase of infant vaccination rate above the present level would be more effective than the promotion of secondary vaccination for an adult age class in order to reduce the infective population.

免疫が一時的であり、失活を伴う場合の単純な伝染病感染動態に関する数理モデル2つ、年齢構造のないものと、3つの年齢グループ（幼年、少年、成年）からなるもの、を考察する。数理モデルには、成人に対するワクチン接種の効果を導入する。特に、具体例として、麻疹感染を取り上げ、麻疹撲滅に対するワクチン接種の効果に関する試論を展開する。数学的解析、および、高知県の人口データおよび麻疹感染データを参照したパラメータ値による数値計算の結果は、幼年期におけるワクチン接種に加えて、成年期でのワクチン接種を行っても、その効果は期待できないということ、ただし、成年期でのワクチン接種が有効であるような人口サイズもありえることを示唆するものである。特に、大きな人口集団における伝染病感染に対しては、ワクチンの2次接種よりも、幼年期でのワクチン接種率の向上が感染者数減少により効果的であると示唆された。

## 1. Introduction

Epidemic dynamics has been attracting not a few theoretical and mathematical researchers (for instance, see [1-5] and their references). In this paper, we analyze two simple mathematical models taking account of the waning immunity, specifically formulated with measles in mind, to give some insight about the effect of vaccination in adult age class according to the elimination of measles within the whole population. First model is non-age-structured one, with which we see the interaction between the immunity waning and the secondary vaccination. Second model is with three age classes: infant, young, and adult. With the model, we discuss the efficiency of adult vaccination for the elimination of measles, with numerical analysis making use of parameter values which could correspond to the demographic situation of a Japanese community, the Kochi Prefecture, which is one of local communities that have experienced some serious outbreaks of measles in several years (see Fig. 1) [6].

In recent Japan, measles cases counts 11,000-22,000 a year in a certain average, and estimated at 286,000 especially for 2001, according to the report of infectious disease surveillance by the Infectious Disease Surveillance Center (IDSC) of the Japanese Ministry of Health, Labour and Welfare [7,8]. More than 60% of the patients in the data are infants below two years old, and more than 95% are

Hiromi SENO [corresponding author]: Department of Mathematical and Life Sciences, Graduate School of Science, Hiroshima University, Higashi-hiroshima 739-8526, JAPAN

e-mail: [seno@math.sci.hiroshima-u.ac.jp](mailto:seno@math.sci.hiroshima-u.ac.jp) Phone & Fax: +81-(0)82-4247394

瀬野裕美 広島大学大学院理学研究科数理分子生命理学専攻 〒739-8526 広島県東広島市鏡山1-3-1

Naoki SATO: Department of Mathematics, Faculty of Science, Hiroshima University, JAPAN

佐藤直樹 広島大学理学部数学科

**Key words:** waning immunity – boosting effect – two-dose vaccination – mathematical model – adult measles

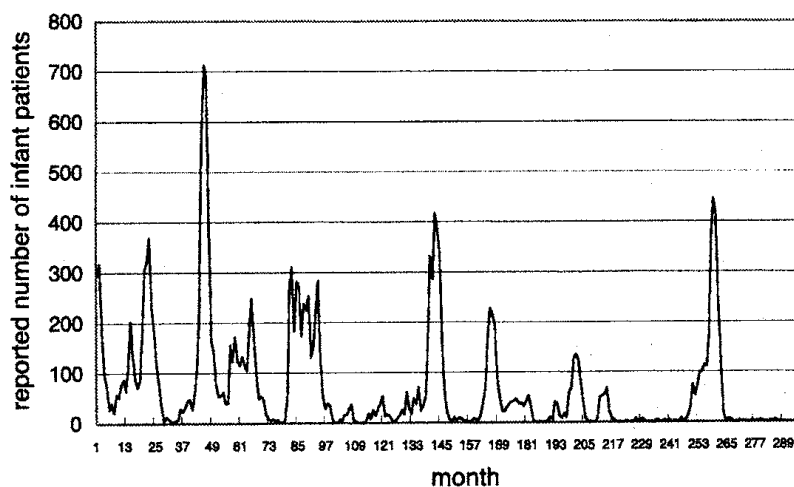


Fig. 1. Number of infant measles cases reported by pediatric sentinel clinics in the Kochi Prefecture, Japan, from July 1979 (the first month) to February 2004 (the 296th month), given by the Kochi Prefectural Infectious Disease Surveillance Center [6].

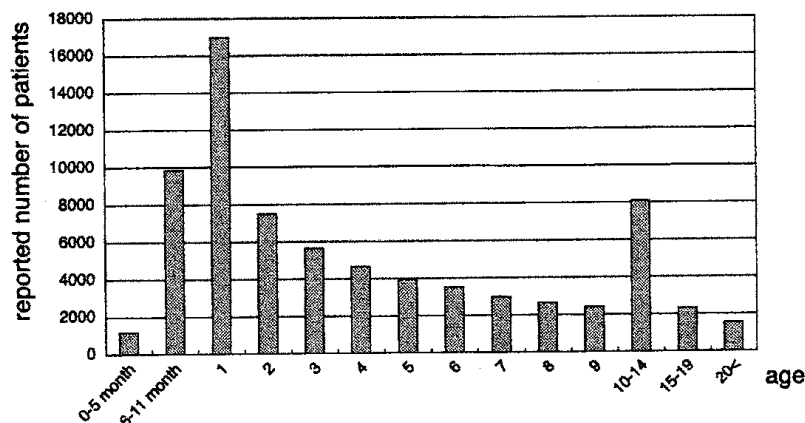


Fig. 2. Age distribution of measles cases in Japan. Drawn by the cumulative data from the 14th week in 1999 to the 29th in 2002 [9].

non-vaccinated. As indicated by Fig. 2, most infected age class is from one to five years old. Every year local outbreak of measles is repeated in Japan [7-9].

Adult measles is defined for patients over 18 years old. Since several years, it has been reported that teenagers vaccinated in the infant period are infected by measles [9,10]. As for the adult measles in Japan, it has no decreasing tendency with about 3-4% of all cases, and the reported number of measles cases decreases in age over 24 years old (see Fig. 3) [8,9].

Today, as seen from Fig. 4, the measles vaccination rate for infants is more than 80% in average over the whole Japan, although there are some local communities with the rate around 50-60% [7-9]. It is said that 3-5% of vaccinated individuals fail to get the immunity [11,12]. On the other hand, the report for the Sapporo City in Japan indicates that around 40% of the measles patients were non-vaccinated [8]. So only such failure of immunization is unsatisfactory to explain the measles infection to vaccinated individuals. It is likely that the effective period of immunity becomes shorter than before. In fact, some sero-epidemiological estimates of antibody decay suggest that 25 years after vaccination, measles antibody levels have waned to below protection levels [13-17]. A hypothesis is that, in past, the immunity was reinforced by re-encountering the pathogen [18-22], what is sometimes called the

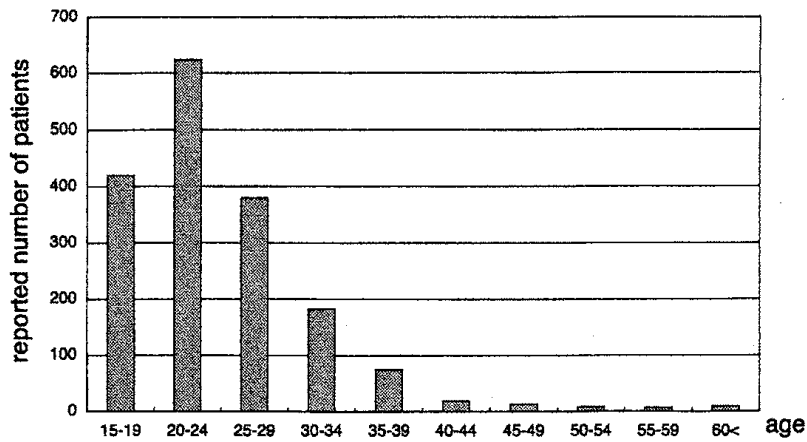


Fig. 3. Age distribution of adult measles cases in Japan. Drawn by the cumulative data from the 14th week in 1999 to the 29th in 2002 [9].

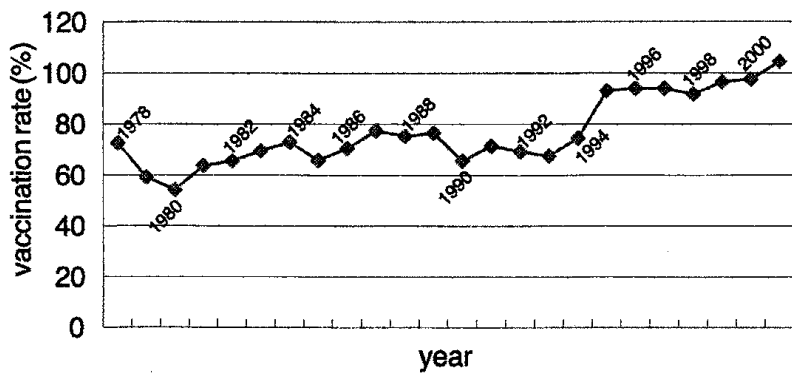


Fig. 4. Measles vaccination rate for infant in Japan [9]. The rate in the data is calculated by the ratio of vaccinated infant population to the population of one year old.

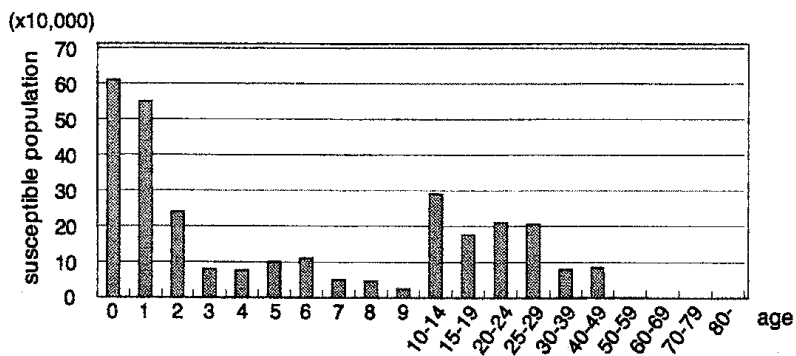


Fig. 5. Estimated number of measles susceptibles in Japan [25]

“boosting effect”, whereas the chance to re-encounter the pathogen recently becomes less and less [23, 24]. Indeed, as shown in Fig. 5, the age distribution of Japanese susceptible population indicates a small peak in teenagers and twenties [25]. Besides, it is said that the Japanese vaccine would be less effective against mutated strains of measles virus [8,9].

Promoting the vaccination program for infants is a possible public health strategy against the measles outbreak. Another strategy is to carry out the secondary vaccination for older age class, which

can be regarded as playing role of an artificial “boosting effect”. Such two-dose vaccination program is recently under consideration for a teenager class in Japan [8,9], while, in the other countries, for example, the United States, Canada, and Australia, it has been promoted for the younger class around or less than 10 years old. Some mathematical models have been analyzed to discuss problems related to such two-dose vaccination schedule [26–30]. In this paper, we consider the secondary vaccination in the adult age class over 18 years old, focusing the adult measles transmission, to get some insights about the efficiency of such two-dose vaccination program for Japanese situation.

## 2. Preliminary Model

### 2.1. Modeling

We consider the epidemic dynamics given by the following SIRM model (see Fig. 6) :

$$\frac{dS}{dt} = -\beta SI - \omega_2 S + \rho_1(I)R + \rho_0(I)M + (1 - \omega_1)bN - \mu S \quad (1)$$

$$\frac{dI}{dt} = \beta SI - \gamma(I)I - \mu I \quad (2)$$

$$\frac{dR}{dt} = \gamma(I)I - \rho_1(I)R - \mu R \quad (3)$$

$$\frac{dM}{dt} = \omega_1 bN + \omega_2 S - \rho_0(I)M - \mu M, \quad (4)$$

where  $S(t)$ ,  $I(t)$ ,  $R(t)$  and  $M(t)$  are respectively the susceptible population, the infective population, the recovered and infection-induced immune population, and the vaccine-induced immune population at time  $t$ . Although not a few models have taken account of latent period [1–3, 31, 32], with an additional subpopulation frequently denoted by  $E$ , exposed to the epidemic disease, we do not consider it in our model.

Parameters  $b$ ,  $\beta$ ,  $\mu$ ,  $\omega_1$ , and  $\omega_2$  are positive constants. Parameter  $b$  is the birth rate,  $\mu$  the natural death rate,  $\beta$  the infection rate. Term  $\beta SI$  introduces the mass-action type of disease transmission from infective to susceptible, like well-known Kermack-McKendrick SIR model [33] (see also [1–3]). Parameter  $\omega_1$  ( $0 \leq \omega_1 \leq 1$ ) is the vaccination rate in the infant period, while  $\omega_2$  ( $0 \leq \omega_2$ ) can be regarded as that in the elder period.

The recovery rate  $\gamma(I)$  is assumed to be a function of infective population density, and so are the immunity waning rates  $\rho_0(I)$  and  $\rho_1(I)$  as well. Vaccine-induced immune individual loses its immunity and comes back to susceptible with rate  $\rho_0(I)$ , while the infection-induced immune individual does with rate  $\rho_1(I)$ . Waning rate of the vaccine-induced immunity is in general less than that of the infection-induced one, as indicated by some serological studies [13–15, 19, 22, 34, 35]. With these  $I$ -dependence, we introduce the boosting effect into our model. As the infective population density gets larger, the recovery of infective individual becomes harder because the infective individual gets more chance for the re-infection of antigen. So the recovery rate averaged over the population is in general decreasing in terms of infective population density. Similarly, the increase of chance for the re-infection of antigen makes the reinforcement of immune system against the antigen, so that the immunity waning rate averaged over the population is decreasing in terms of infective population density.

We consider a stationary population, that is, a constant total population  $N = S + I + R + M$  at any time  $t$ . Hence, from (1–4), at any time  $t$ ,

$$\frac{dN}{dt} = \frac{dS}{dt} + \frac{dI}{dt} + \frac{dR}{dt} + \frac{dM}{dt} = (b - \mu)N = 0.$$

Therefore, we assume  $\mu = b$  hereafter.

### 2.2. Disease-free Equilibrium

From (1–4), we can easily find that the disease-free equilibrium ( $S^*$ ,  $I^* = 0$ ,  $R^* = 0$ ,  $M^* = N - S^*$ ) always exists, where

$$S^* = \frac{(1 - \omega_1)b + \rho_0(0)}{b + \rho_0(0) + \omega_2} N.$$

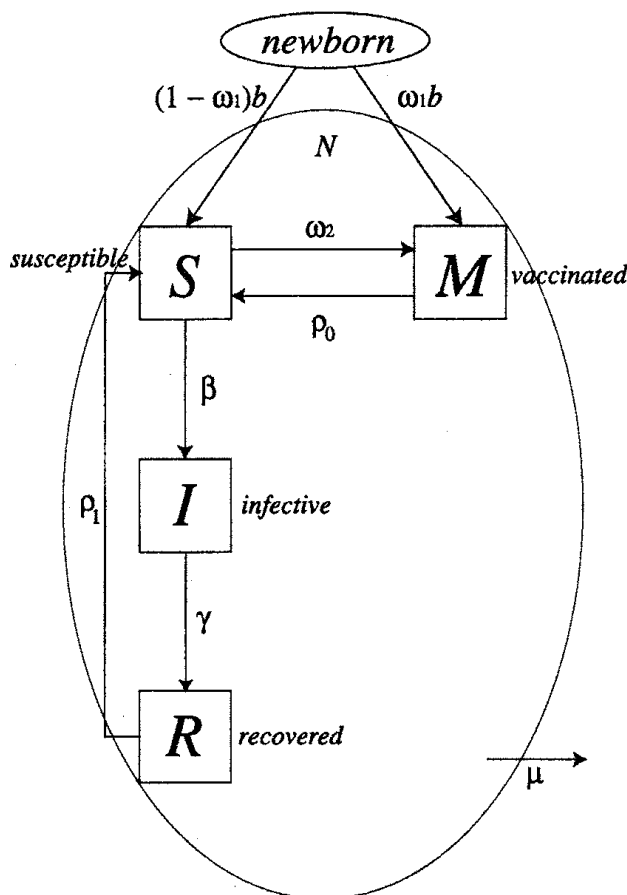


Fig. 6. SIRM model (1-4).

By means of the standard eigenvalue analysis, we can easily obtain the following condition for its locally asymptotic stability:

$$N < \frac{\{b + \rho_0(0) + \omega_2\}\{b + \gamma(0)\}}{\{(1 - \omega_1)b + \rho_0(0)\}\beta} = N_c^*. \quad (5)$$

For the population of size  $N > N_c^*$ , the epidemic disease eventually becomes endemic. This result simultaneously means that the *basic reproductive number*  $R_0$  is given by

$$R_0 = \frac{\{(1 - \omega_1)b + \rho_0(0)\}\beta N}{\{b + \rho_0(0) + \omega_2\}\{b + \gamma(0)\}}. \quad (6)$$

Disease-free equilibrium is asymptotically stable if  $R_0 < 1$ , while it is unstable if  $R_0 > 1$ . The basic reproductive number  $R_0$  is monotonically increasing in terms of  $\rho_0(0)$ , that is,  $R_0$  becomes larger as the wane of immunity gets faster. However,  $R_0$  does not infinitely increase but has the upper bound  $N/N_{c1}$ , where

$$N_{c1} = \frac{\gamma(0) + b}{\beta}.$$

From the condition (5), as shown by Fig. 7, we can see three different cases: i) the disease-free equilibrium can be asymptotically stable even without any vaccination; ii) only the infant vaccination can bring the disease-free equilibrium even without secondary vaccination; ii) the secondary vaccination is necessary for the disease elimination.

The first case corresponds to the sufficiently small size of total population such that  $N \leq N_{c1}$ . In this case, the condition (5) is satisfied for any pair of  $\omega_1$  and  $\omega_2$ . Besides, as mentioned for the



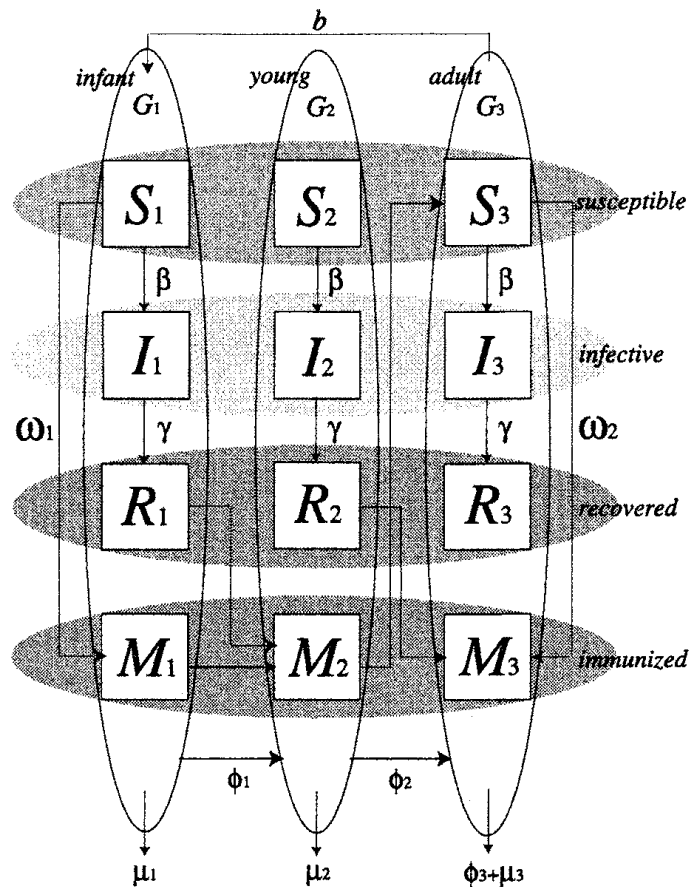


Fig. 8. Three age class model (11–22). As for the detail explanation, see text.

We remark that these results are independent of mathematical detail features of functions  $\gamma(I)$  and  $\rho_i(I)$  ( $i = 0, 1$ ) except for values  $\gamma(0)$  and  $\rho_0(0)$ . Therefore, our results are valid for a family of functions for  $\gamma(I)$  and  $\rho_i(I)$  ( $i = 0, 1$ ).

When the disease-free equilibrium is unstable, the system approaches some endemic state. Depending of the detail features of  $I$ -dependence of functions  $\gamma(I)$  and  $\rho_i(I)$  ( $i = 0, 1$ ), the detail features of endemic state, such as its bifurcation structure, could appear mathematically interesting even for our simple model. However, we do not analyze them here, and will present elsewhere. In this paper, we are focusing the invasion of epidemic disease, so that the main subject is the local stability of disease-free equilibrium. If the disease-free equilibrium is asymptotically stable, we translate the situation as that an invading small infective population decreases toward zero and its invasion fails. Otherwise, the invading infective population increases and occurs an outbreak of disease transmission.

### 3. Three Age Class Model

#### 3.1. Modeling

#### POPULATION DYNAMICS

Now, we construct a mathematical model with three age classes: infant age class (Group 1) from age 0 to  $a_1$ , young age class (Group 2) from age  $a_1$  to  $a_2$ , and adult age class (Group 3) from age  $a_2$  to  $a_3$  (see Fig. 8).

Let us consider the susceptible, the infective, the recovered, and the vaccinated/immunized subpopulations in each age class ( $i = 1, 2, 3$ ):

$S_i(t)$  : the susceptible population in Group  $i$  at time  $t$ ;  
 $I_i(t)$  : the infective population in Group  $i$  at time  $t$ ;  
 $R_i(t)$  : the recovered population in Group  $i$  at time  $t$ ;  
 $M_i(t)$  : the vaccinated or immunized population in Group  $i$  at time  $t$ ;  
 $G_i(t)$  : the population size of each age class at time  $t$ :  $G_i(t) = S_i(t) + I_i(t) + R_i(t) + M_i(t)$ .

Especially  $M_1$  means the vaccinated infant population. In contrast,  $M_2$  includes the individuals vaccinated in the infant age class and those recovered from the infection in the infant age class. We assume that those who can get the immunity in the infant age class can carry an effective immunity even in the young age class, and becomes susceptible in the adult age class because of the waning immunity. We introduce the secondary vaccination in the adult age class. Hence,  $M_3$  includes the individuals recovered from the infection in the young age class and those vaccinated in the adult age class.

We consider the population dynamics governed by the following system:

$$\frac{dS_1}{dt} = bG_3 - \lambda_1(I_1, I_2, I_3)S_1 - \omega_1S_1 - \phi_1S_1 - \mu_1S_1 \quad (11)$$

$$\frac{dI_1}{dt} = \lambda_1(I_1, I_2, I_3)S_1 - \gamma_1I_1 - \phi_1I_1 - \mu_1I_1 \quad (12)$$

$$\frac{dR_1}{dt} = \gamma_1I_1 - \phi_1R_1 - \mu_1R_1 \quad (13)$$

$$\frac{dM_1}{dt} = \omega_1S_1 - \phi_1M_1 - \mu_1M_1 \quad (14)$$

$$\frac{dS_2}{dt} = -\lambda_2(I_1, I_2, I_3)S_2 + \phi_1S_1 - \phi_2S_2 - \mu_2S_2 \quad (15)$$

$$\frac{dI_2}{dt} = \lambda_2(I_1, I_2, I_3)S_2 - \gamma_2I_2 + \phi_1I_1 - \phi_2I_2 - \mu_2I_2 \quad (16)$$

$$\frac{dR_2}{dt} = \gamma_2I_2 - \phi_2R_2 - \mu_2R_2 \quad (17)$$

$$\frac{dM_2}{dt} = \phi_1(M_1 + R_1) - \phi_2M_2 - \mu_2M_2 \quad (18)$$

$$\frac{dS_3}{dt} = -\lambda_3(I_1, I_2, I_3)S_3 - \omega_2S_3 + \phi_2(S_2 + M_2) - \phi_3S_3 - \mu_3S_3 \quad (19)$$

$$\frac{dI_3}{dt} = \lambda_3(I_1, I_2, I_3)S_3 - \gamma_3I_3 + \phi_2I_2 - \phi_3I_3 - \mu_3I_3 \quad (20)$$

$$\frac{dR_3}{dt} = \gamma_3I_3 - \phi_3R_3 - \mu_3R_3 \quad (21)$$

$$\frac{dM_3}{dt} = \omega_2S_3 + \phi_2R_2 - \phi_3M_3 - \mu_3M_3, \quad (22)$$

where the disease infection force functions  $\lambda_i$  ( $i = 1, 2, 3$ ) are given by

$$\lambda_i(I_1, I_2, I_3) = \beta_{i1}I_1 + \beta_{i2}I_2 + \beta_{i3}I_3.$$

Parameters  $b$ ,  $\phi_i$ ,  $\beta_{ij}$ ,  $\gamma_i$ ,  $\mu_i$ ,  $\omega_1$ , and  $\omega_2$  ( $i, j = 1, 2, 3$ ) are all positive constants. Meaning of each parameter is given in Table 1. As indicated in (11), the net birth rate is proportional to the population size  $G_3$  of Group 3. We assume that any reproductive individual belongs to Group 3.

#### ASSUMPTION OF CONSTANT POPULATION SIZE

We assume that the population size of each age class,  $G_i$  ( $i = 1, 2, 3$ ), is temporally constant, that is, assume a stationary age class distribution. Eventually, the total population size  $N = G_1 + G_2 + G_3$  is also assumed constant. By this assumption, the following equations must be satisfied according to (11–22):

$$\frac{dG_1}{dt} = bG_3 - (\mu_1 + \phi_1)G_1 = 0 \quad (23)$$

Table 1. Parameter list in the three age class model (11–22).

$b$	birth rate
$\mu_i$	natural death rate in Group $i$
$\phi_i$	population transfer rate from Group $i$ to the subsequent age class
$\beta_{ii}$	infection rate within the same Group $i$
$\beta_{ij} (i \neq j)$	infection rate from Group $j$ to Group $i$
$\gamma_i$	recovery rate of the infective in Group $i$
$\omega_1$	vaccination rate in the infant age class
$\omega_2$	vaccination rate in the adult age class

$$\frac{dG_2}{dt} = \phi_1 G_1 - (\mu_2 + \phi_2) G_2 = 0 \quad (24)$$

$$\frac{dG_3}{dt} = \phi_2 G_2 - (\mu_3 + \phi_3) G_3 = 0. \quad (25)$$

## BALANCE EQUATIONS

Next, we consider the population renewal in the infant age class. As indicated in (11), the newborn population  $bG_3\Delta t$  enters into the infant age class during  $[t, t + \Delta t)$ . This cohort of newborn population decreases to  $bG_3e^{-\mu_1 a_1}\Delta t$  at time  $t + a_1$  with the natural death of rate  $\mu_1$ . On the other hand, population  $\phi_1 G_1\Delta t$  of age  $a_1$  is transferred from Group 1 to Group 2 during  $\Delta t$ . Thus, we obtain the following equation:

$$bG_3e^{-\mu_1 a_1}\Delta t = \phi_1 G_1\Delta t. \quad (26)$$

In the same way, we can get the similar equations for each age class:

$$\phi_1 G_1 e^{-\mu_2(a_2 - a_1)}\Delta t = \phi_2 G_2\Delta t; \quad (27)$$

$$\phi_2 G_2 e^{-\mu_3(a_3 - a_2)}\Delta t = \phi_3 G_3\Delta t. \quad (28)$$

From these equations (26–28), we can obtain the expression for  $\phi_1$ ,  $\phi_2$ , and  $\phi_3$  with the other parameters:

$$\phi_1 = b \frac{G_3}{G_1} e^{-\mu_1 a_1} \quad (29)$$

$$\phi_2 = b \frac{G_3}{G_2} e^{-\{\mu_1 a_1 + \mu_2(a_2 - a_1)\}} \quad (30)$$

$$\phi_3 = b e^{-\{\mu_1 a_1 + \mu_2(a_2 - a_1) + \mu_3(a_3 - a_2)\}}. \quad (31)$$

With the assumption of a stationary age class distribution, those equations (23–25) and (29–31) give the following relation between birth rate  $b$  and death rates  $\mu_1$ ,  $\mu_2$ , and  $\mu_3$ :

$$b = \frac{\mu_3 e^{\mu_1 a_1 + \mu_2(a_2 - a_1)}}{1 - e^{-\{\mu_3(a_3 - a_2)\}}}. \quad (32)$$

Since the total population size  $N$  is constant, from (23–25) and (29–31), we can obtain the following equations, too:

$$\frac{G_1}{N} = \frac{b\mu_2(1 - e^{-\mu_1 a_1})}{b\mu_2(1 - e^{-\mu_1 a_1}) + b\mu_1 e^{-\mu_1 a_1}(1 - e^{-\mu_2(a_2 - a_1)}) + \mu_1\mu_2} \quad (33)$$

$$\frac{G_2}{N} = \frac{b\mu_1 e^{-\mu_1 a_1}(1 - e^{-\mu_2(a_2 - a_1)})}{b\mu_2(1 - e^{-\mu_1 a_1}) + b\mu_1 e^{-\mu_1 a_1}(1 - e^{-\mu_2(a_2 - a_1)}) + \mu_1\mu_2} \quad (34)$$

$$\frac{G_3}{N} = \frac{\mu_1\mu_2}{b\mu_2(1 - e^{-\mu_1 a_1}) + b\mu_1 e^{-\mu_1 a_1}(1 - e^{-\mu_2(a_2 - a_1)}) + \mu_1\mu_2}. \quad (35)$$

Consequently, for given natural death rates  $\mu_i$  ( $i = 1, 2, 3$ ), the birth rate  $b$  is uniquely determined by (32), and then, from (33–35), ratios  $G_i/N$  ( $i = 1, 2, 3$ ) are determined, and vice versa. Further, from (29–31), population transfer rates  $\phi_i$  ( $i = 1, 2, 3$ ) are determined, too.

Table 2. Parameter values for numerical calculation

Parameter	Original data/relation	Used value
$G_1$	33,910 *	35,182
$G_2$	123,705 *	90,289
$N$	813,949 *	820,000
$a_1$	—	5
$a_2$	—	18
$a_3$	—	$\infty$
$\bar{b}$	Equation (32)	$1.0 \times 10^{-2}$ (/year)
$\mu_1$	Equations (23–25)	$5.2 \times 10^{-3}$ (/year)
$\mu_2$	Equations (23–25)	$7.0 \times 10^{-9}$ (/year)
$\mu_3$	Equations (23–25)	$1.0 \times 10^{-2}$ (/year)
$\phi_1$	Equation (29)	$2.0 \times 10^{-1}$ (/year)
$\phi_2$	Equation (30)	$6.7 \times 10^{-2}$ (/year)
$\phi_3$	Equation (31)	0 **
$\gamma_1 = \gamma_2 = \gamma_3$	1/(9 days)	40.6 (/year)
$J$	Equation (36)	7,073

\*Data of the Kochi Prefecture in Japan, 2000.

\*\*Group 3 consists of every individual over 18 years old.

### 3.2. Parameters for Numerical Calculation

For our three age class model, we analyze it mainly with numerical calculations, making use of measles data for the Kochi Prefecture in Japan [6]. Parameter values used for numerical calculations are given in Table 2.

#### AGE CLASS

In Japan, the infant measles infection occurs mostly from one to five years old [9], so that we put  $a_1 = 5$ . Since the adult measles infection is defined for individual over 18 years old in Japan, we put  $a_2 = 18$ , and  $a_3 = \infty$  in our model. Therefore, Group 3 consists of every individual over 18 years old.

#### BIRTH RATE, DEATH RATE, AND POPULATION TRANSFER RATE

In our model, the population renewal is assumed proportional to the population size  $G_3$ . In contrast, given 'birth rate'  $\bar{b}$  in the demographic data is generally defined by the ratio of newborn numbers to the total population  $N$ . Hence, we get the following relation between  $\bar{b}$  and  $b$ :

$$b = \bar{b} \cdot \frac{N}{G_3}.$$

From a demographic data for  $\bar{b}$  in Japan [37], we roughly choose the parameter value of  $b$  as in Table 2.

With the estimated value of  $b$ , we can numerically estimate values of  $\mu_1$  and  $\mu_2$  from (33–35), then can get the value of  $\mu_3$  from (32). As for the population transfer rate  $\phi_3$ , we put  $\phi_3 = 0$  because Group 3 consists of every individual over 18 years old. From (29–31), we can obtain values of  $\phi_1$  and  $\phi_2$ .

#### RECOVERY RATE

We assume that the mean duration of infection till recovery is common for any infective individual, independently of age. From the general knowledge about the measles infection, we put the mean duration of infection 9 days. Therefore, from  $\gamma_i = \gamma = 1/9$  ( $i = 1, 2, 3$ ) per day, we can get the value of  $\gamma$  per year in Table 2.

Table 3. Infection rate for numerical calculation.

Infection rate	Value/year
$\beta_{11}$	$1.3 \times 10^{-3}$
$\beta_{12} = \beta_{21} = \beta_{22}$	$2.5 \times 10^{-4}$
$\beta_{13} = \beta_{23} = \beta_{33} = \beta_{32} = \beta_{31}$	$3.3 \times 10^{-6}$

### INFANT VACCINATION RATE

In the surveillance data, the vaccination rate  $\tilde{\omega}$  is defined by the ratio of vaccinated infant population to the population of one year old. On the other hand, the measles vaccination for Japanese infant is scheduled at present for those from twelve to ninety months after birth. In this reason, the vaccination rate  $\tilde{\omega}$  in the surveillance data can be beyond 100% (see Fig. 4).

In our numerical calculation, we give the population of one year old,  $J$ , by

$$J = \int_1^2 bG_3 e^{-\mu_1 t} dt = \frac{bG_3(e^{-\mu_1} - e^{-2\mu_1})}{\mu_1}. \quad (36)$$

Then, at an equilibrium state with the equilibrium value  $M_1^*$ , we assume that  $\tilde{\omega} = M_1^*/J$ . If the vaccination rate in data is 80%, we use the correspondence such that  $M_1^*/J = 0.8$ .

At the equilibrium state for our model, we can get the expression of  $M_1^*$  from (11-14) as follows:

$$M_1^* = \frac{\omega_1 \{bG_3 - (\gamma_1 + \phi_1 + \mu_1)I_1^*\}}{(\phi_1 + \mu_1)(\omega_1 + \phi_1 + \mu_1)}. \quad (37)$$

Hence, for instance, according to the surveillance data for the Kochi Prefecture in 2002 and 2003 [6], except for years when the measles infection outbreaks, if we put  $I_1^* = 16$ , then, with  $\tilde{\omega} = M_1^*/J = 0.8$ , we can get the infant vaccination rate  $\omega_1 = 4.483 \times 10^{-2}$ .

According to the disease-free equilibrium with parameter values in Table 2, making use of (37) with  $I_1^* = 0$ , we can numerically calculate the correspondence between  $\tilde{\omega}$  and  $\omega_1$ :  $\omega_1 = 2.856 \times 10^{-2}$  for  $\tilde{\omega} = 0.6$ ,  $\omega_1 = 3.411 \times 10^{-2}$  for  $\tilde{\omega} = 0.7$ ,  $\omega_1 = 3.993 \times 10^{-2}$  for  $\tilde{\omega} = 0.8$ ,  $\omega_1 = 4.604 \times 10^{-2}$  for  $\tilde{\omega} = 0.9$ , and  $\omega_1 = 5.246 \times 10^{-2}$  for  $\tilde{\omega} = 1.0$ .

With parameter values in Table 2,  $\tilde{\omega}$  becomes beyond 100% at relatively small value of  $\omega_1$ . Besides, the value of  $\tilde{\omega}$  significantly depends on the infective population size  $I_1^*$ :  $\tilde{\omega}$  becomes beyond 100% with  $I_1^*$  more than about 132. This indicates that, even for relatively small infective population size  $I_1^*$ , the vaccination rate  $\tilde{\omega}$  corresponding to that in the demographic data is beyond 100%.

### INFECTION RATE

If we apply those infection rates used in [38],  $\beta_{11} = 2.4 \times 10^{-4}$ ,  $\beta_{12} = \beta_{21} = \beta_{22} = 2.6 \times 10^{-4}$ , and  $\beta_{13} = \beta_{23} = \beta_{33} = \beta_{32} = \beta_{31} = 1.3 \times 10^{-4}$ , our numerical calculation with  $\omega_2 = 0$  and  $\omega_1 = 4.483 \times 10^{-2}$  which is derived in case of  $I_1^* = 16$  and  $\tilde{\omega} = M_1^*/J = 0.8$  with (37), indicates a fluctuation around  $(I_1, I_2, I_3) \approx (16, 100, 200)$  in the stationary state. According to the case of the Kochi Prefecture ([6], and see Fig. 1), the corresponding values averaged over recent several years result in  $(I_1 + I_2, I_3) \approx (16, 1)$ , which seems much smaller than the above numerical result. So we turned infection rates so that those values of  $(I_1, I_2, I_3)$  at the stationary state have order corresponding to the data for the Kochi Prefecture, and as a result we choose those values in Table 3.

#### 3.3. Disease-Free Equilibrium

As for the local stability analysis for the disease-free equilibrium, we carry it out with numerically calculating its eigenvalues with those parameter values in Tables 2 and 3. Our numerical calculations show that the eigenvalues for the disease-free equilibrium are all real for any  $\omega_1$  and  $\omega_2$ .

## CRITICAL VACCINATION RATE

At first, let us consider a specific case with  $\omega_2 \rightarrow \infty$ . This is the case when the adult vaccination is perfectly carried out so that no susceptible individual exists in Group 3 at any time  $t$ . So  $S_3 = 0$  at the disease-free equilibrium, too. In this case, the numerically obtained maximal eigenvalue is 22.526 with  $\omega_1 = 0.0$ , and  $-29.907$  with  $\omega_1 = 1.0$ . It is numerically shown that the maximal eigenvalue is monotonically decreasing in terms of  $\omega_1$ . As a result, we find that, even with the perfect vaccination in the adult age class, there exists a critical value  $\omega_{1C}$  for  $\omega_1$  such that the disease-free equilibrium is asymptotically stable with  $\omega_1 > \omega_{1C}$ , and unstable with  $\omega_1 < \omega_{1C}$ . We can numerically obtain  $\omega_{1C} = 0.11367$  in this case.

With  $\omega_{1C} = 0.11367$ , we can numerically calculate the value of  $M_1^*$  by (37) at the disease-free equilibrium, and obtain  $\tilde{\omega} = M_1^*/J = 175.08\%$  with the population size  $J$  in Table 2.

Next, we consider another specific case with  $\omega_2 = 0$ , when the adult vaccination is not carried out at all. This case corresponds to the present situation in Japan. In the same way as for the previous case, we can numerically obtain the maximal eigenvalue, 22.541 with  $\omega_1 = 0.0$ , and  $-29.888$  with  $\omega_1 = 1.0$ . Compared to the maximal eigenvalue with  $\omega_2 \rightarrow \infty$ , the difference is very small:  $10^{-2}$ – $10^{-1}\%$  in order. Indeed, the  $\omega_1$ -dependence of maximal eigenvalue is rather similar with that for the case of  $\omega_2 \rightarrow \infty$ , so that the difference is negligible. The critical value  $\omega_{1C}$  in this case is numerically obtained as  $\omega_{1C} = 0.11379$ , and correspondingly  $\tilde{\omega} = 175.20\%$ .

On the other hand, we can consider another specific case with  $\omega_1 \rightarrow \infty$ . This is the case when the infant vaccination is perfectly carried out. In this case, no susceptible individual exists in Group 1 at any time  $t$ , and eventually no susceptible also in Group 2 at any time  $t$  because of the effective immunity. We can explicitly obtain the analytical expression of every eigenvalue for the disease-free equilibrium, and get the general condition for its asymptotic stability as follows:

$$\omega_2 > \frac{\phi_3 + \mu_3}{\phi_3 + \mu_3 + \gamma_3} \cdot \{\beta_{33}G_3 - (\phi_3 + \mu_3 + \gamma_3)\}, \quad (38)$$

where we used the equations (23–25). This condition means the existence of case when the adult vaccination could be essential for the elimination of disease. However, only in case when the right side of (38) is positive, that is, when the population size  $G_3$  of adult age class is sufficiently great beyond a specific size, this condition could be meaningful. Indeed, in our case with parameter values given in Tables 2 and 3, the right side of (38) has a negative value, so that the perfect vaccination in the infant age class leads to the disease-free state, independently of the adult vaccination. Making use of (35), we can numerically estimate the population size with which the condition (38) is meaningful:  $G_3 > 1.236 \times 10^7$  that corresponds to the condition that the total population size  $N > 1.453 \times 10^7$ . This result implies that a huge community with population over ten million could never reach the disease-free state only with the infant vaccination, whereas the secondary vaccination program might be effective to eliminate the disease or decrease the infective population.

Consequently, our numerical calculations indicate that, almost independently of the value of  $\omega_2$ , the population approaches the disease-free equilibrium if the infant vaccination rate  $\omega_1$  is beyond a critical value, whereas it approaches the endemic state if  $\omega_1$  is below the critical value.

## EFFECT OF TOTAL POPULATION SIZE

Critical value  $\omega_{1C}$  for the vaccination rate  $\omega_1$  depends on the total population size  $N = G_1 + G_2 + G_3$ . We numerically investigated the maximal eigenvalue for the disease-free equilibrium with parameter values of Tables 2 and 3 except for population sizes, and found that the critical value  $\omega_{1C}$  has an almost linear dependence on the total population size.

Also in these numerical investigations, the contribution of  $\omega_2$  to the result appears negligible. Indeed, even in the specific case of  $\omega_2 \rightarrow \infty$ , the critical size of total population is  $5.277 \times 10^5$  with  $\omega_1 = 0$  and  $3.099 \times 10^6$  with  $\omega_1 = 1$ , while, in case of  $\omega_2 = 0$ ,  $5.276 \times 10^5$  with  $\omega_1 = 0$  and  $3.094 \times 10^6$  with  $\omega_1 = 1$ .

In Table 4, we show numerically obtained critical infant vaccination rate in terms of the total population size. We conclude that it would be hard for the population over eight hundred thousands to reach the disease-free equilibrium with the present level of infant vaccination rate, while the population

Table 4. Critical infant vaccination rate versus the total population size in case of  $\omega_2 = 0$ .

Total population size ( $\times 10^5$ )	$\omega_{1C}$	Corresponding $\tilde{\omega}$ (%)
< 5.276	0.00000	0.000
6.000	0.02818	59.304
6.010	0.02856	60.000
6.152	0.03411	70.000
6.302	0.03993	80.000
6.624	0.05246	100.000
7.000	0.06709	121.014
8.000	0.10600	167.296
9.000	0.14492	203.293
10.000	0.18384	232.092
100.000	3.73842	465.589

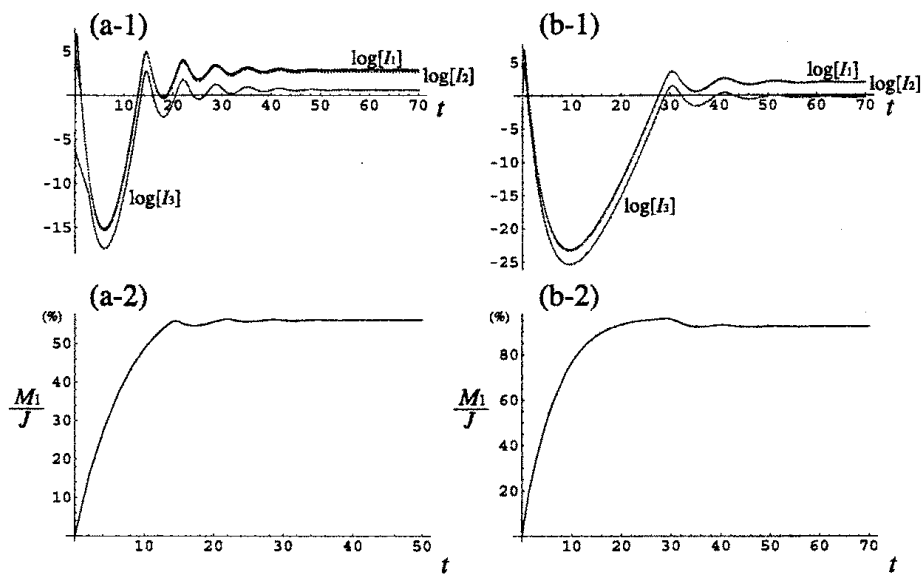


Fig. 9. Temporal variation toward the endemic state. Numerically calculated with parameter values given in Tables 2 and 3 with  $\omega_2 = 0$ . Initial conditions are given by  $S_1(0) = G_1 - 76$ ,  $I_1(0) = 76$ ,  $S_2(0) = G_2 - 224$ ,  $I_2(0) = 224$ ,  $S_3(0) = G_3$ , and  $I_3(0) = R_i(0) = M_i(0) = 0$  ( $i = 1, 2, 3$ ), which correspond to the data for the Kochi Prefecture [6]. (a)  $\omega_1 = 3.0 \times 10^{-2}$ ; (b)  $\omega_1 = 5.0 \times 10^{-2}$ . (a-1) and (b-1) show the temporal variation of infective populations in logarithmic value. (a-2) and (b-2) show that of the corresponding ratio  $M_1/J$ .

below seven hundreds thousands is likely to reach the disease-free equilibrium. Furthermore, small population below five hundreds thousands would eventually reach the disease-free equilibrium without any vaccination.

## ENDEMIC STATE

As indicated by our numerical calculations in the previous section, with the present level of infant vaccination rate, the population over seven hundred thousands would be on the way toward endemic state. In our numerical calculations, such endemic state was always an equilibrium approached through dumping oscillation with rather large amplitude, as shown in Fig. 9. Such nature of dumping oscillation may be involved in typical repetitive outbreaks of measles as seen also for the case of the Kochi Prefecture in Japan (Fig. 1). Characteristics of the dumping oscillation is sensitively affected by the value of  $\omega_1$  in our numerical calculations. We found such a tendency that the frequency of oscillation becomes smaller as  $\omega_1$  gets larger.

#### 4. Conclusion

Our results for both non-age-structured and three age class models clearly indicate that the vaccination program should be planned with taking account of the size of population within which the disease transmission is taking place. It is expected that the vaccination program would be effective to reduce drastically the incidence within relatively small population, whereas it could not eliminate the repeated outbreak of infection within relatively large population as in some Japanese local communities [7–9].

Especially with the present level of infant vaccination rate in Japan, it is likely that the measles elimination would be far away from its realization. Besides, in case of Japan, the secondary vaccination program for an adult age class would be little effective, compared to the promotion program of infant vaccination. Although our numerical calculations imply that it would be hard to increase the infant vaccination rate enough to make the population approach the measles-free equilibrium, the increase of infant vaccination rate above the present level would be at least more effective than the secondary vaccination for an adult age class in order to reduce the infective population.

For a relatively large population, the promotion of both infant vaccination and secondary vaccination for an adult age class would be the proper strategy for the public health. In such case, the selection of age class targeted by the secondary vaccination would be one of the most important factors which determine the result of vaccination program. Many mathematical modeling considerations have studied this subject [26–30]. However, as Guris [24] mentioned for the limited population of Palau, we remark here that, for a relatively small population, such two-dose vaccination program would not be necessarily more appropriate than the promotion of single dose vaccination program. Moreover, for a sufficiently large population, the two-dose vaccination program would be less effective than the promotion program of primary vaccination.

Although our models have mathematically simple structure with mass-action type of disease transmission, we conjecture that, except for the detail bifurcation structure of solution, the essential feature of solution would be similar to that for some SEIR model or even for the more sophisticated or complicated model with a range of corresponding parameter values.

*Acknowledgements.* The authors greatly thank Prof. Masayuki Kakehashi for his valuable comments and encouragement to complete this work.

#### References

1. R.M. Anderson and R.M. May, *Infectious Diseases of Humans: Dynamics and Control*, Oxford University Press, Oxford, 1991.
2. F. Brauer and C. Castillo-Chávez, *Mathematical Models in Population Biology and Epidemiology*, Texts in Applied Mathematics 40, Springer, New York, 2001.
3. O. Diekmann and J.A.P. Heesterbeek, *Mathematical Epidemiology of Infectious Diseases: Model Building, Analysis and Interpretation*, Wiley Series in Mathematical and Computational Biology, John Wiley & Son, Chichester, 2000.
4. J.D. Murray, *Introduction to Mathematical Biology*, Interdisciplinary Applied Mathematics 17, Springer, New York, 2002.
5. J.D. Murray, *Mathematical Biology: Spatial Models and Biomedical Applications, 3rd Edition*, Interdisciplinary Applied Mathematics 18, Springer, New York, 2002.
6. 高知県健康福祉部健康政策課, 高知県における麻疹流行と取組報告, 高知, 2003年3月.
7. Infectious Disease Surveillance Center (IDSC), Measles, Japan, 1999–2001, *Infectious Agents Surveillance Report (IASR)* **22**(11): 273–274 (2001).
8. Infectious Disease Surveillance Center (IDSC), Measles, Japan, 2001–2003, *Infectious Agents Surveillance Report (IASR)* **25**(3): 60–61 (2004).
9. 国立感染症研究所 感染症情報センター, 麻疹の現状と今後の麻疹対策について, 東京, 2003年10月.
10. WHO, WHO guidelines for epidemic preparedness and response to measles outbreaks, pp. 35–36, Geneva, Switzerland, 1999.
11. B.S. Hersh, L.E. Markowitz, R.E. Hoffman, et al., A measles outbreak at a college with prematriculation immunization requirement, *Am. J. Public Health*, **81**: 360–364 (1991).
12. A. Vaisberg, J.O. Alvarez, H. Hernandez, et al., Loss of maternally acquired measles antibodies in well-nourished infants and response to measles vaccination: Peru, *Am. J. Public Health*, **80**: 736–738 (1990).
13. B. Christenson and M. Bottiger, Measles antibody — comparison of long-term vaccination titers, early vaccination titers and naturally acquired-immunity to and booster effects on the measles virus, *Vaccine*, **12**: 129–133 (1994).

14. R.T. Chen, L.E. Markowitz, P. Albrecht, et al., Measles antibody — reevaluation of protective titers, *J. Infect. Dis.*, **162**: 1036-1042 (1990).
15. L.E. Markowitz, S.R. Preblid, P.E.M. Fine, et al., Duration of live measles vaccine-induced immunity, *Pediatr. Infect. Dis. J.*, **9**: 101-110 (1990).
16. J. Mossong, D.J. Nokes, W.J. Edmunds, et al., Modeling the impact of subclinical measles transmission in vaccinated populations with waning immunity, *Am. J. Epidemiol.*, **150**: 1238-1249 (1999).
17. J. Mossong, C.J. O'Callaghan, and S. Ratnam, Modelling antibody response to measles vaccine and subsequent waning of immunity in a low exposure population, *Vaccine*, **19**: 523-529 (2001).
18. J. Bennett, H. Whittle, B. Samb, et al., Seroconversions in unvaccinated infants: Further evidence for subclinical measles from vaccine trials in Niakhar, Senegal, *Int. J. Epidemiol.*, **28**: 147-151 (1999).
19. R.F. Helfand, D.K. Kim, H.E. Gary, et al., Nonclassic measles infections in an immune population exposed to measles during a college bus trip, *J. Med. Virol.*, **56**: 337-341 (1998).
20. S. Huiss, B. Damien, F. Schneider, et al., Characteristics of asymptomatic secondary immune response to measles virus in late convalescent donors, *Clin. Exp. Immunol.*, **109**: 416-420 (1997).
21. I.R. Pedersen, C.H. Mordhorst, G. Glikmann, et al., Subclinical measles infection in vaccinated seropositive individuals in arctic Greenland, *Vaccine*, **7**: 345-348 (1989).
22. J. Mossong and C.P. Muller, Modelling measles re-emergence as a result of waning of immunity in vaccinated populations, *Vaccine*, **21**: 4597-4603 (2003).
23. K. Glass and B.T. Grenfell, Antibody dynamics in childhood disease: Waning and boosting of immunity and the impact of vaccination, *J. theor. Biol.*, **221**: 121-131 (2003).
24. D. Guris, J. McCreedy, J.C. Watson, et al., Measles vaccine effectiveness and duration of vaccine-induced immunity in the absence of boosting from exposure to measles virus, *Pediatr. Infect. Dis. J.*, **15**: 1082-1086 (1996).
25. 多屋馨子, 新井智, 松永泰子, 岡部信彦, 2000年度麻疹血清疫学調査ならびにワクチン接種率調査～感染症流行予測調査より～, *Infectious Agents Surveillance Report (IASR)* **22(11)**: 275-277 (2001).
26. R.M. Anderson and R.M. May, Age-related changes in the rate of disease transmission: Implication for the design of vaccination programmes, *J. Hygiene*, **94**: 365-436 (1985).
27. J.M. Dreesman, An array based simulation approach for predicting the impact of different measles vaccination strategies in Lower Saxony, *APL Quote Quad*, **31**: 5-12 (2001).
28. N.J. Gay, L. Pelletier, and P. Duclos, Modelling the incidence of measles in Canada: An assessment of the options for vaccination policy, *Vaccine*, **16**: 794-801 (1998).
29. V. Roudersfer and N.G. Becker, Assessment of two-dose vaccination schedules: Availability for vaccination and catch-up strategies, *Math. Biosci.*, **129**: 41-66 (1995).
30. D. Schenzle, An age-structured model of pre- and post-vaccination measles transmission, *IMAJ Math. Appl. Med. Biol.*, **1**: 169-191 (1984).
31. C.J. Duncan, S.R. Duncan, and S. Scott, The dynamics of measles epidemics, *Theor. Pop. Biol.*, **52**: 155-163 (1997).
32. P.E.M. Fine, Herd immunity: History, theory, practice, *Epidemiol. Rev.*, **15**: 265-304 (1993).
33. W.O. Kermack and A.G. McKendrick, A contribution to the mathematical theory of epidemics, *Philos. R. Soc. Lond. A* **115**: 700-721 (1927).
34. C.P. Mueller, Measles elimination: Old and new challenges?, *Vaccine*, **19**: 2258-2261 (2001).
35. C.P. Mueller, F. Fack, B. Damien, et al., Immunogenic measles antigens expressed in plants: Role as an edible vaccine for adults, *Vaccine*, **21**: 816-819 (2003).
36. W. Katzmann and K. Dietz, Evaluation of age-specific vaccination strategies,, *Theor. Pop. Biol.*, **25**: 125-137 (1984).
37. 総務省統計局, 年報, 平成 15 年 10 月 1 日現在推計人口, 東京, 2004 年 3 月.
38. H.R. Babad, D.J. Nokes, N.J. Gay, et al., Predicting the impact of measles vaccination in England and Wales: Model validation and analysis of policy options, *Epidemiol. Infect.*, **114**: 319-344 (1994).